Available online at www.sciencedirect.com
ScienceDirect
Progress in Natural Science 19 (2009) 195–203
Progress in Natural Science
www.elsevier.com/locate/pnsc

Improved retracking algorithm for oceanic altimeter waveforms

Lifeng Bao *, Yang Lu, Yong Wang

Institute of Geodesy and Geophysics, Chinese Academy of Sciences, Wuhan 430077, China

Received 14 March 2008; received in revised form 4 June 2008; accepted 16 June 2008

Abstract

Over the deep oceans without land/ice interference, the waveforms created by the return altimeter pulse generally follow the ocean model of Brown, and the corresponding range can be properly determined using the result from an onboard tracker. In the case of complex altimeter waveforms corrupted due to a variety of reasons, the processor on the satellite cannot properly determine the center of the leading edge, and range observations can be in error. As an efficacious method to improve the precision of those altimeter observations with complex waveforms, waveform retracking is required to reprocess the original returning pulse. Based on basic altimeter theory and the geometric feature of altimeter waveforms, we developed a new altimeter waveform retracker, which is valid for all altimeter waveforms once there exists a reasonable returning signal. The performances of the existing Beta-5 retracker, threshold retracker, improved threshold retracker, and the new retracker are assessed in the experimental regions (China Seas and its adjacent regions), and the improvements in the accuracy of sea surface height are investigated by the difference between retracked altimeter observations and referenced geoid. The comparisons denote that the new algorithm gives the best performance in both the open ocean and coastal regions. Also, the new retracker presents a uniform performance in the whole test region. Besides, there is a significant improvement in the short-wavelength precision and the spatial resolution of sea surface height after retracking process.

Keywords: Altimetry; Waveform retracking; Sea surface height

1. Introduction

As a very successful technique, satellite altimetry has now been used for some 30 years and yielded some important results. It has also become a standard tool for geophysicists, including oceanographers, geodesists, and solid earth physicists [1]. The basic concept of satellite altimetry is deceptively straightforward. Over the oceans, the altimeter transmits a short pulse of microwave radiation with known power toward the sea surface. The pulse interacts with the rough sea surface, and part of the incident radiation reflects back to the altimeter. From the time for the pulse to travel a round trip and the time for returning waveform, the satellite altimeter will provide the measurement of the range from the satellite to the sea surface, the significant wave height and the backscatter coefficient of the sea surface in real-time.

Most marine applications of satellite altimetry begin with sea surface height (SSH). A SSH of altimetry is derived from the satellite's orbital height, and the range observations between the antenna and the sea surface are determined using the altimeter waveforms. Over the deep seas without land/ice interference, the waveforms created by the returning altimeter pulse generally follow the ocean model of Brown [2], and the corresponding range observations can be properly determined using the result from an onboard tracker. However, near coasts, altimeter waveforms may be corrupted due to a variety of reasons, and the range observations can be in error. For example, such corruptions of waveforms in ERS and Envisat altimetry over global coastal zones have been presented in Ref. [3].

* Corresponding author. Tel./fax: +86 27 86783841.
E-mail address: baolifeng@asch.whigg.ac.cn (L. Bao).

1002-0071/$ - see front matter © 2008 National Natural Science Foundation of China and Chinese Academy of Sciences. Published by Elsevier Limited and Science in China Press. All rights reserved.
doi:10.1016/j.pnsc.2008.06.017

Ref. [4] estimated that TOPEX/Poseidon waveforms are corrupted over waters about 20 km from the shore around southern Australia. Use of erroneous altimeter ranges may lead to false results in such applications as gravity anomaly determination and sea level change studies. Further improvement in the accuracy and resolution of the marine gravity field will require more precise altimeter measurements and/or a longer duration mission to minimize the various noise sources [5].

To improve the precision of those altimeter observations with complex returning waveforms, a waveform retracker is required to reprocess the original returning pulse. The altimeter waveform retracker is defined as one algorithm for determining the correction by the tracking gate bias. And the retracked SSH is defined as a SSH which, in addition to standard geophysical and instrument corrections [1], is corrected by the tracking gate bias determined from waveform retracking. Recent efforts [5–7] have shown that the use of retracked SSHs has improved the determination of gravity anomaly over coastal waters and the open ocean.

On the whole, the methods of waveform retracking can be classified into three categories: one is based on functional fit, one is based on statistics, and the other is based on analyzing sub-waveforms. The review of the first two retracking methods can be found in Refs. [8,9]. The third retracking method can be found in Refs. [7,10]. Refs. [6,8,11] also reported the development of a waveform classification procedure (or expert system) to select the optimum retracker for retracking all waveforms. However, few studies have been done on developing an all-purpose retracker applicable for all kinds of waveforms.

In this paper, we propose an alternative improved retracking algorithm capable of retracking waveform with reasonable returning signals. The improvements in SSH determination are investigated with respect to existing retracking algorithms in the test regions (China Seas and its adjacent regions). It is revealed that the new retracker performs best in retrieving SSH observations, and presents a uniform performance in the whole test regions. Furthermore, the new retracker does not require any previous restriction, and no smoothness constraint on arrival times along the satellite's ground track is needed. We will show an initial result to demonstrate the improvement and discuss the future enhancements.

2. Data and area

The data used in this study are ERS-1 altimeter waveform product (ALT.WAP), which is a level 1.5 product and contains all the information telemetered in the altimeter source packets together with the corrections, calibration and orbit data required to further process the data into higher level geophysical products. This product has the same general content as the level 1.0 waveform foundation product (ALT.WDR), and is updated if the following optional data are available: the precision orbit-derived location data to replace the restituted orbit-derived data; the improved calibration corrections to replace the coarse corrections; the improved wet tropospheric corrections to be inserted; and geoid and tidal information. The altimeter waveform is provided in a set of power signals with respect to time at 64 sample bins (or gates).

The ERS-1 mission effectively consists of a combination of several different missions. In all ERS-1 waveform datasets, the geodetic mission (GM) enables the acquisition of a high density of altimeter measurements, and thus improves the determination of the marine SSH. In this study, nearly 3 years of 20 Hz ERS-1 GM waveform data from ALT. WAP products were used in a region close to China bounded by 100–145 E and 0–45 N. The bathymetry and coastal geometry in the test regions are rather diverse, and different degrees of waveform corruption are expected. Fig. 1 shows the geographical distribution of the observations in this study.

As the original purpose of this study was to investigate the improvement of SSH determination in the coastal regions characterized by shallow water (depth $<$200 m), we draw the contour of ocean depth 200 m in Fig. 2. Here, open ocean (depth $>$200 m) was painted with blue color, and the distance between ocean depth 200 m and the real coastline alters from several kilometers to hundreds of kilometers.

For assessing the performance of all retrackers in the test region, we estimated the SSH before and after retracking by adopting the standard processing steps (algorithms) and the same geophysical corrections (including dry tropospheric correction, wet tropospheric corrections, ionospheric corrections, ocean tidal corrections, earth tidal corrections, ocean loading tidal corrections, dopper range corrections and spacecraft offset corrections), except the different retracking corrections. Considering the SST characteristic in South China Sea and the possible variety of

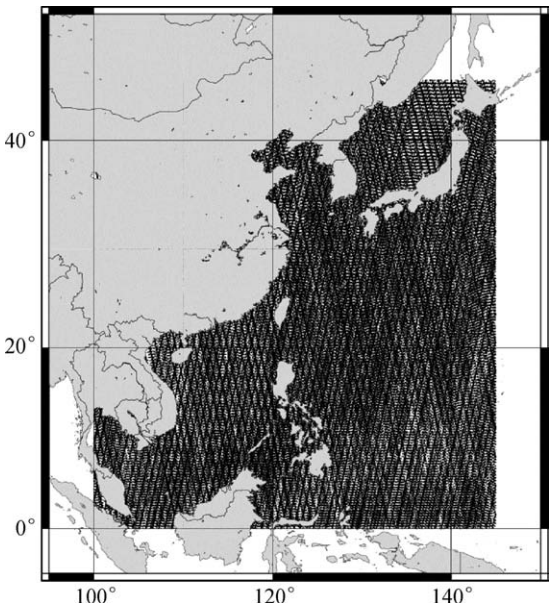

Fig. 1. Ground tracks of ERS WAP data.

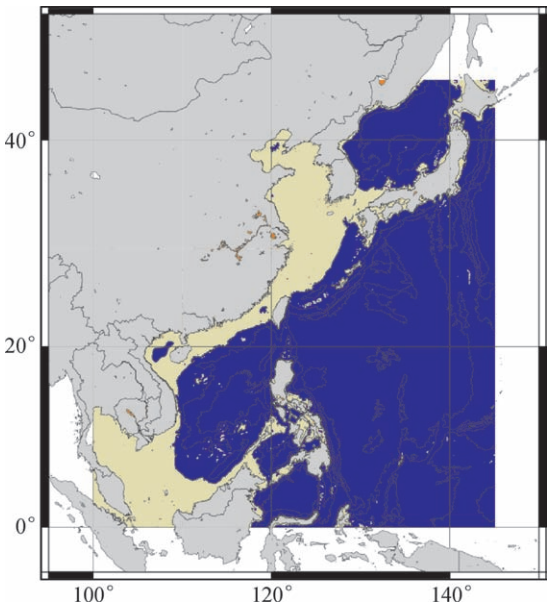

Fig. 2. Bathymetry and coastal geometry in China seas and their adjacent areas.

post-retracking SSH in 1 s, we removed those gross-errors exceeding ±5 m in sea surface topography (1 Hz) and ±1 m in the difference between 20 Hz SSH observations and its average 1 s for raw SSH and all retrackers.

3. Methods

3.1. Waveform retracking

The simplified work principle of the satellite altimetry is as follows: the radar altimeter emits a short pulse which is a frequency-modulated chirp that reflects from the ocean surface and returns to the antenna. The recorded power is the double convolution of the system point target response with the ocean surface height distribution and the two-way antenna pattern. If the point target response is approximated with a Gaussian form, the height distribution of ocean waves is well approximated by a Gaussian function [12]. Then, the form of the return power is well approximated by an error function with a slow decay of the trailing edge due to the finite antenna beam width

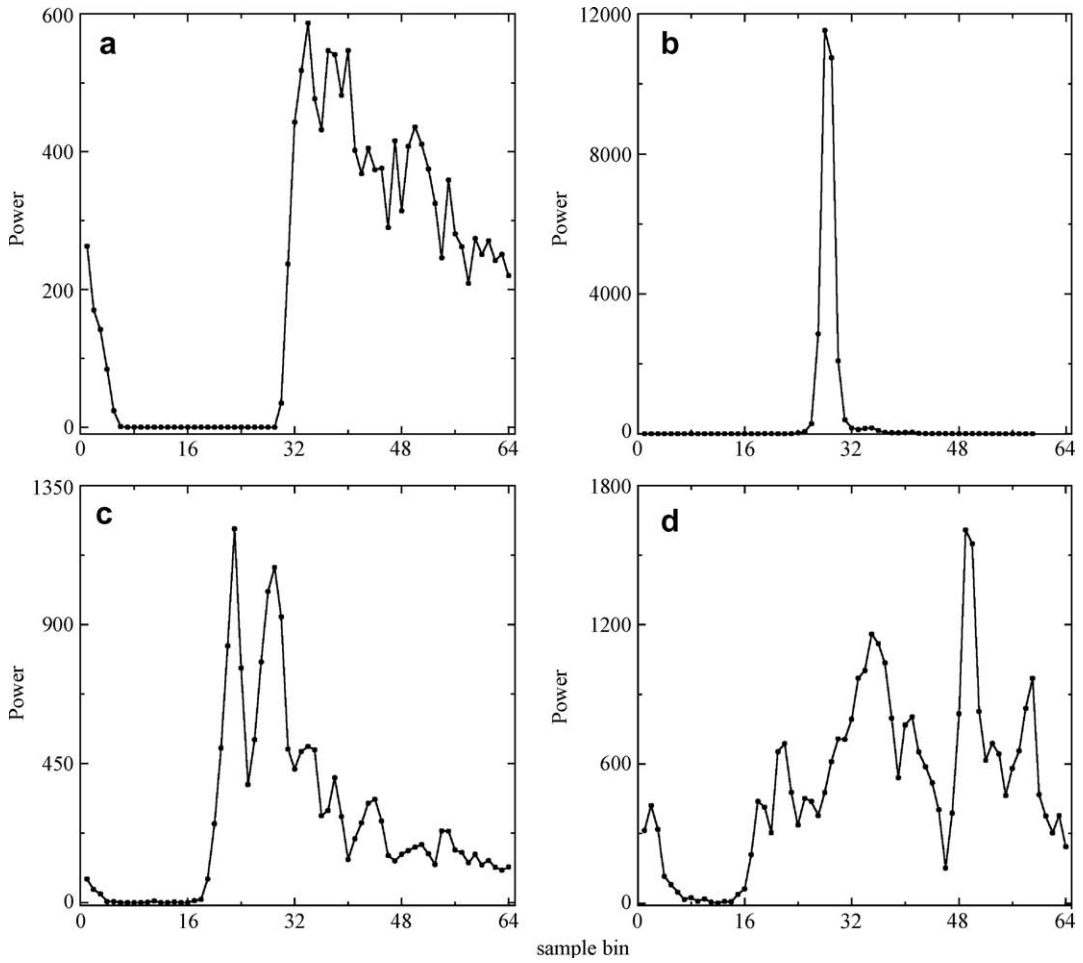

Fig. 3. Sample return waveform. (a) Ocean waveform; (b) ice waveform; (c) multi-peak waveform; (d) complex waveform.

[13]. A basic model of the radar return from the ocean surfaces was constructed by Ref. [2], and has been widely used in the altimetry community [14–16].

Generally, individual open ocean echo corresponds well to a mathematical model, which enables precise range to surface information to be retrieved. Waveforms are assumed to follow the functional form of Brown [2]. However, echoes in coastal/ice zones are frequently distorted and therefore fail the standard automated processing procedures, and are rejected [6]. Fig. 3 shows some sample waveforms of ERS-1. The first waveform is a typical ocean waveform, following the Brown model; the second one is waveform in ice region, called ice waveform, which differs from the Brown model significantly; the third is a multi-peak waveform that appeared near the coastline; and the last one is a complex waveform, which is often rejected or leads to error correction in most of the retrackers, but is still accepted for the new retracker. For both the normal and complex waveforms, the predefined tracking gate of 32.5 (mid-gate used by ERS-1 onboard tracker) does not match the leading edges of waveforms in most cases. Thus, the retracking process is required for improving the range precision of existing measurements.

Waveform retracking is defined as an algorithm which finds the mid-gate of leading slope in the return waveform, and then corrects the range measurements from the on-satellite tracking algorithm according to the departure between the mid-gate and original measurement [17].

3.2. Improved retracking algorithm

For any altimeter satellite/mission, there is one universal principle in all reasonable return waveforms: once signal reflection produces one leading edge, there is always at least one leading edge in the return waveform. This conclusion is supported by a rigorous statistical analysis of hundreds of millions of return waveforms, and is also validated by those representative return waveforms, shown in Fig. 3. Consequently, once we find one leading edge, we can determine the retracking gate and compute the retracking correction corresponding to this reflection.

In theory, there is only one leading edge that corresponds to the true observational reflection from the sea surface in the return waveform – the power of the returning pulse increases from zero to some maximum value over a time interval of about 6–60 ns. For the purpose of estimating the sea surface height, the only waveform parameters of interest are the return travel time and the electromagnetic bias. Travel time estimates can be optimized by concentrating on the exact location of the leading edge, and the electromagnetic bias can be derived from backscatter in trailing edge, which will be discussed in another paper. In this paper, we will prove the improvement in SSH by determining the retracking correction from travel time, and will not discuss the influence from geophysical corrections, such as atmospheric correction or ocean tidal correction. Since

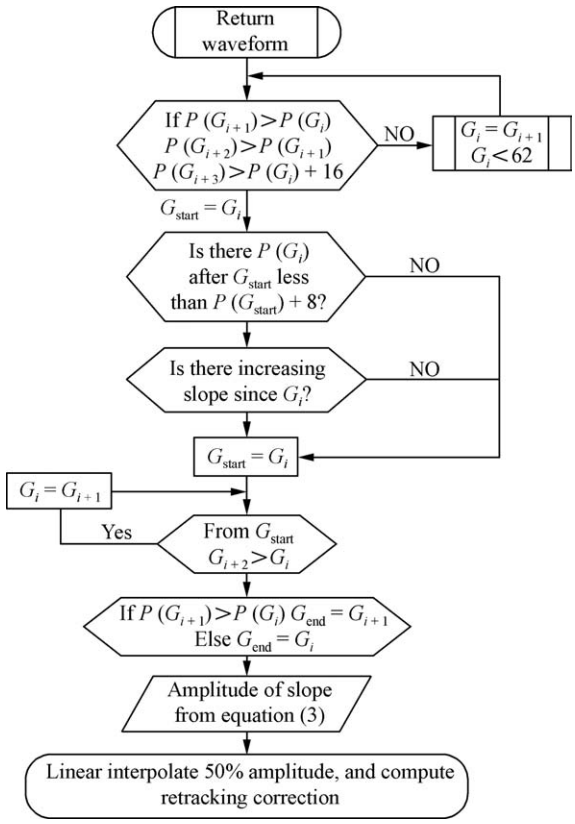

Fig. 4. Flowchart of the new improved retracking algorithm.

we used referenced electromagnetic correction, the retracking correction will only be relative to the leading edge.

Without attempting to explain the full shape of the waveform, we were only interested in finding the right leading edge of the waveform that corresponds to the true observational physical process (sea surface reflection). Fig. 4 shows the flowchart of our improved retracking algorithm, which determines the retracking gate according to the following procedure: first, we searched the "start gate", from which there was an increasing slope continuing to at least two gates. The difference between the powers of two successive gates was computed. If the increment was greater than a given precision of return power (empirical value 8 for ERS waveform), then it showed that the onboard antenna began to pick up the returning power, and recorded the power as the "start power". If there were other "start powers", we would select the smallest one among the first value and other records adding the given precision. And, the corresponding gate was recorded as the "start gate". From the "start gate" determined by the above steps, the difference between the gate and the gate after next was computed until the difference was smaller than zero. The increasing slope in the return waveform indicated that the antenna continued to pick up the returning power. Finally, the power of the last gate, used in the above computation, and the power of the one before were compared, and the larger one was recorded as the "end power". The corresponding gate was recorded as the "end gate". Thus, the slice between the "start gate" and

the "end gate" was determined as the leading slope with respect to the true sea surface reflection. The leading edge derived from the above rigorous criteria is creditable and accurate, because this searching procedure for the leading edge is agreed with the observational process of altimeter waveform theory.

Generally, there are only 2–10 bin widths (or gates) in the leading slope. So, it is difficult to determine the retracking gate by the method of functional fit from the selected slice. It is acceptable to use improved threshold algorithm. To determine the retracking gate, the amplitude of the selected slope will be estimated with the following formula:

$$Amp = \sqrt{\frac{\sum P(G_i)^4}{\sum P(G_i)^2}} \tag{1}$$

where Amp is the amplitude, $P(G_i)$ is the power at gate G_i, and i is the number of sample bin. In computation, those return powers from G_{start} to G_{end+4} are used in Eq. (1). At the final step, the retracking gate is determined by estimating the location of bin with half of the amplitude. For altimeter waveforms, the retracking correction will be

$$Retracking\_corr = \frac{c\tau}{2}(retracking\_gate - 32.5) \tag{2}$$

where c is the speed of light; τ is the pulse duration, and 32.5 is the original mid-gate from onboard tracker. For ERS-1, $\tau = 3.125$ ns.

The principle of the improved retracker is simple and applicable for all satellites. So the new retracker will work in all cases once there are reasonable return waveforms (existing leading edge). For those waveforms with no leading edge, caused by several reasons, no retracking gate should be derived in theory. Unfortunately, those cases have not been refused by other retrackers and there are still output (obviously, those results are unacceptable). However, such cases will always be refused by the new retracker.

3.3. Comparison with existing retracking algorithms

We have compared the improved retracking algorithm with three existing representative retrackers. The three existing retrackers are (i) method of functional fit: Beta-5 retracker. Refs. [18,19] give details of the associated partial derivatives and a weighting scheme in the least-squares solution. (ii) A modified threshold retracking method: Offset Center of Gravity (OCOG) [16,20]. This method estimates the amplitude, width, and center of gravity of the waveform, then determines the retracking gate with a predefined threshold value. Here, the modified threshold retracking method employs the threshold value 50% to determine the retracking gate. (iii) Improved threshold retracker, which determines one or more sub-waveforms and retracking gates, and then selects a best retracking gate, which yields the smallest difference between the post-retracking SSH and previous referenced data [7,10].

Essentially, the kernel of any retracker algorithm is to find the true leading edge in the return waveform. When we try to fit the return waveform with some given reference model/function, the most important parameter (rise-time) in the fit process will be contaminated by the other parts of the waveform except the leading edge. Though given that different prior weights to each sample of the waveform can be used to reduce the effect from other parts, the least-squares fit and regression algorithm are sensitive to the prior weight and the initial referenced model. We have to determine the prior weight based on type, characteristic and geographical location of the return waveform. In fact, there is no standard reference model function that can be used for all cases. In the retracking process, those retrackers based on the functional fit will be sensitive to the shape of return waveform, and there is no guarantee of convergence in the least-squares solution.

Furthermore, the assumption that rise-time parameter varies smoothly along the satellite's ground track is not always right, especially in the coastal regions and Polar region. The decay parameter controlling the trail edge is not constant along the track either. The retracker based on statistics is usually used in deep seas, though the result from this retracker seems "smoother" than those from other retrackers, caused partly by the smoothing assumption and filtering technique. The assumption will break down as the waves approach depths comparable to their wavelength ~300 m, since the amplitudes will increase and the wavelength will shorten over distances related to the bathymetric gradient [13]. Those retrackers based on the assumption of continuity will also be sensitive to the distribution of waveforms. For recovering those complex waveforms, which is also the major motivation of retracking, we have to regard each return waveform as an independent observation.

Instead of constructing a waveform model, the improved threshold retracker only focuses on the geometry characterization of the return waveform, which determines one or more sub-waveforms and retracking gates, and then selects a best retracking gate according to referenced data and previous SSH. The current post-retracking SSH will be compared with the previous SSH or referenced data (e.g. artificial SSH, geoid add tide model, used in Ref. [10]) associated with the computed retracking gates to make a decision: the "best" retracking gate is the one that yields the smallest difference between the current SSH and previous SSH (or referenced data) [7,10]. Obviously, these improved threshold retrackers are sensitive to the accuracy of the referenced data and previous data to a great extent. It will work properly in the open ocean, but may fail when missing or wrong referenced data are used. In some cases, a wrong previous SSH or discontinuous observations may lead to a false result for all subsequent observations.

Starting from the above retrackers, the new retracker we propose is not only associated with the physical process of the return waveform, but also associated with the geometric feature of the return waveform. Compared with the existing retracking algorithms, the new retracker is just

related to the leading edge of the waveform, and will not be influenced by the other parts of waveform. On the other side, the new retracker regards each waveform as an independent case, and there is no assumption about the relativity to the consecutive waveforms. Though compared with the improved threshold retracker in Refs. [7,10], there seems a little quantitative change in searching the leading slope, it is really a qualitative change in the theory. The key of the former is how to "select" a retracking gate according to the referenced data, and the key of the latter is how to "find" the right retracking gate. Profited from the rigorous criteria associated with the real physical process of sea surface reflection in searching a right slope, there is always only one retracking gate outputted, and no previous referenced data for selecting sub-waveform or previous SSH are needed. Therefore, the retracking corrections from the new retracker will really be objective and independent. In some complex cases, the complex waveform may be rejected by other retrackers or when no referenced data are valid, the new retracker will still work properly.

As a numerical example of our improved retracker, Fig. 5 shows one short section of the post-retracking SSHs from retrackers and corresponding referenced geoid profile in the Taiwan Strait. Given this short time, the true SSH should be as smooth as geoid profile. However, due to a variety of reasons, there are obviously wrong observations in raw SSHs. Clearly the predefined tracking gates in two corrupted waveforms are not the center points of the leading edges. In this case, the retracking process is required for retrieving reasonable SSH observations. Using different retrackers, we can obtain different retracking gates. One detailed example in determining the retracking gates for corrupted waveforms is shown in Fig. 5.

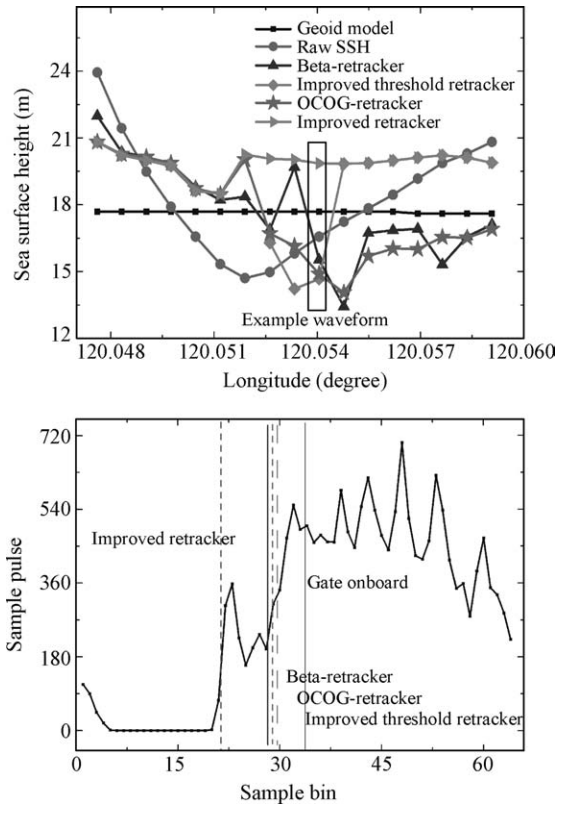

Fig. 5. Comparison of retracked SSHs and referenced geoid height (top) and retracking gates from different retrackers (bottom).

To present the optimum retracker, the performance of retrackers was also investigated in quantity by computing the standard deviations of the difference between SSHs and geoidal heights, and improvement percentage (IMP) of retracked SSHs. The IMP is defined as

$$\mathrm{IMP} = \frac{\sigma_{\mathrm{raw}} - \sigma_{\mathrm{retracked}}}{\sigma_{\mathrm{raw}}} \times 100\% \tag{3}$$

where σ_{raw} and $\sigma_{\mathrm{retracked}}$ are the standard deviations of the differences between raw SSHs and geoidal heights, and the retracked SSHs and geoidal heights, respectively. Table 1 shows the performance of SSHs from raw and retrackers. A small standard deviation indicates that this SSH is more reasonable. The comparison reported in Table 1 suggests that our improved retracker performs best in retrieving these distorted observations. IMP of the new tracker is up to 77.9%, and the standard deviation of post-retracking SSH is only 0.565 m. It should be indicated that the IMP is only significant for short SSH profiles or small areas. Given a long SSHs profile or a large area, the IMP will be controlled by the value of σ_{raw}, which may be a large value due to the variety of sea surface topographies, and the difference between σ_{raw} and $\sigma_{\mathrm{retracked}}$ will be smaller along with the increment of statistical samples. After all, retracking is required for a few cases. In such cases, the IMPs from retrackers may be a same small value, and it will be difficult to assess the performance of retrackers.

4. Results and discussion

A lack of independent datasets to absolutely assess the performance of different retrackers (there are no such independent datasets, because the SSH from altimeter is really average height of bighting area), in this study, we compared the results from different retrackers in more detail – the 20-Hz post-retracking SSH in open ocean and in the coastal regions will be compared with referenced geoid, respectively.

To present the optimum retracker, we used a pre-established criterion to assess the performance of retrackers: For those normal waveforms, the best retracker will give the least noise to the SSH determination, it means that the post-retracking SSH should be as smooth as the SSH profile before retracking; for those complex waveforms, the post-retracking SSH from the best retracker should be smoother than the raw SSH profile. In addition, the optimum retracker should present the same performance (uniform accuracy for post-retracking SSH) both in open ocean and in the coastal regions.

Fig. 6 shows one experimental ground track (totaling 8082 waveforms), its corresponding geoid profile, and 20-Hz post-retracking SSH profiles derived from different retrackers. In the figure, the ocean depth was derived by

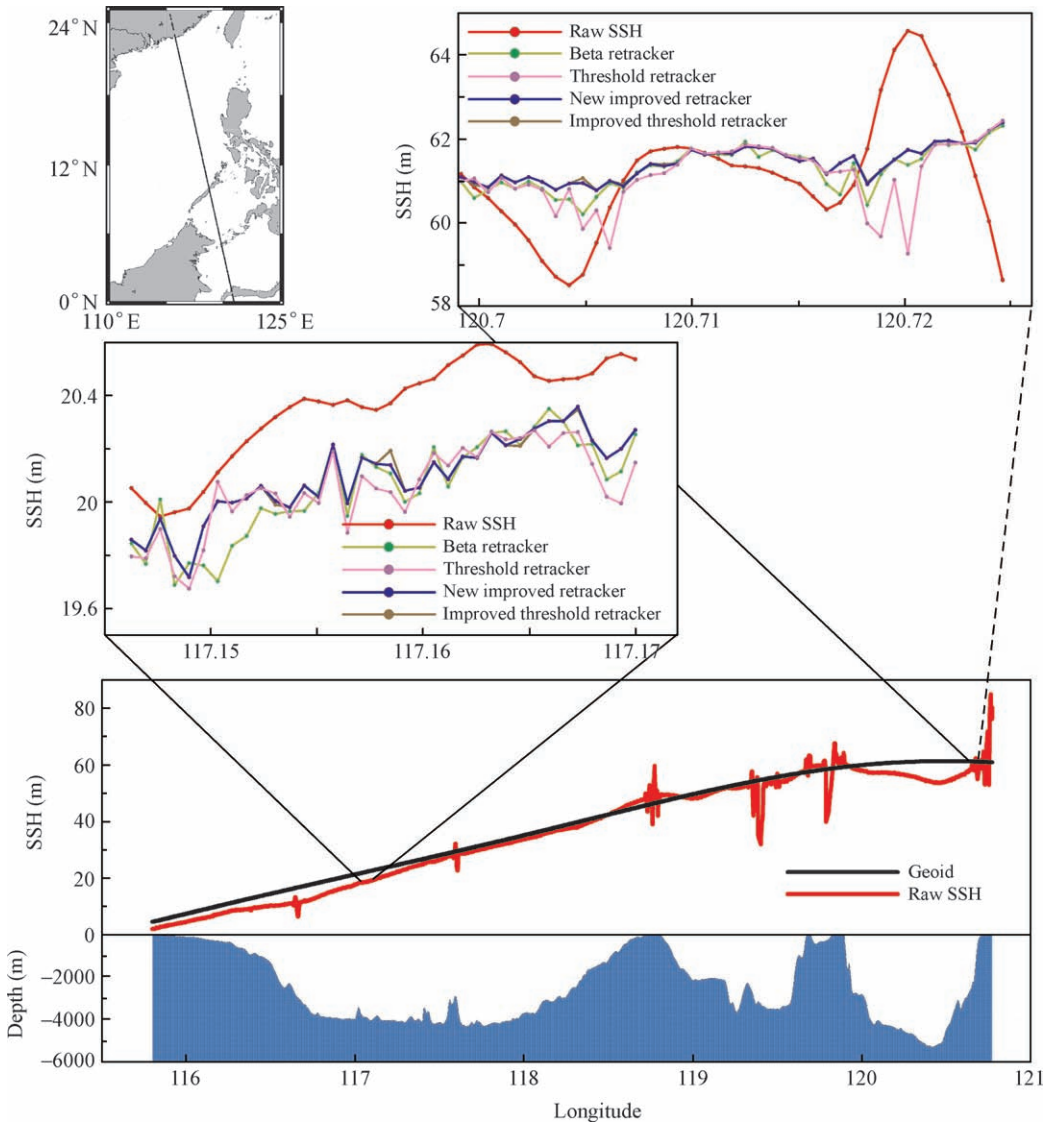

Fig. 6. Comparison between post-retracking SSH from retrackers and referenced geoid height in experimental regions. The altimeter track in the South China Sea is indicated in the upper left figure.

interpolating the ETOPO2 (Earth Topography) datasets. Given the varying depth and the complicated coastal geometry in the test regions, different degrees of waveform corruption were expected. Consequently, the comparison between SSH profiles from retrackers and referenced geoid gave us a creditable result to assess all the retracking algorithms.

Essentially, the difference between post-retracking SSH and referenced geoid height is composed of two parts: one is the contribution of sea surface topography (SST) and the other comes from the high-frequency noise, which denotes the roughness of post-retracking SSH. The first component could be estimated by computing the difference between geoid and the average SSH in 1 s, and the latter was estimated by computing the difference between 20-Hz post-retracking SSHs and its average SSH in 1 s.

Table 2 shows the performance in the above two components from different retrackers, and the statistics of the comparison. The data reported in Table 2 suggest that there are great improvements in the accuracy of SST after retracking both in open ocean and in shallow water, except for the Beta-5 retracker. It confirms that the retracking algorithm is a useful method to improve the precision of

Table 1
A numerical example of improvement from retrackers.

	Number after removing gross error	SD (m)	IMP (%)
Raw[a]	17	2.552	/
Retracker I[b]	17	2.153	15.6
Retracker II[c]	15	2.127	16.7
Retracker III[d]	17	2.100	17.7
Retracker IV[e]	17	0.565	77.9

[a] Raw SSH.
[b] Beta-retracker.
[c] Improved threshold retracker.
[d] OCOG-retracker.
[e] Improved retracker.

Table 2
Comparison of improvement from retrackers for one experimental track (unit: m).

	Depth (>200 m)			Depth (10–200 m)		
	SST std.	Noise std.	Total std.	SST std.	Noise std.	Total std.
One track in the South China Sea						
Raw[a]	2.083	0.152	2.088	2.232	0.208	2.242
Retracker I[b]	2.056	0.171	2.063	2.473	0.189	2.480
Retracker II[c]	2.037	0.171	2.044	2.229	0.177	2.236
Retracker III[d]	2.055	0.170	2.062	2.194	0.201	2.203
Retracker IV[e]	2.022	0.159	2.028	2.175	0.159	2.181

[a] Raw SSH.
[b] Beta-retracker.
[c] Improved threshold retracker.
[d] OCOG-retracker.
[e] Improved retracker.

altimetry observations. With the new improved retracker, such improvement was found in open ocean from 2.083 to 2.022 m. In the coastal regions, the improvement in SST was from 2.232 to 2.175. The failure of the Beta-5 retracker in the coastal regions could be explained as that the real return waveform in shallow water did not follow the ideal Brown model, which was applicable for the waveforms in the open ocean.

To find the optimal retracker, comparison of performances of retrackers was carried out for more altimeter tracks. In total, 2215 altimeter tracks (14,604,595 waveforms) were investigated, and the detailed comparison is shown in Table 3 (for ground tracks, see Fig. 2). In this study, the statistical comparison between different retrackers was performed with the following parameters: the number of reasonable SSHs (after removing gross-errors with predefined editorial criterion), the number of raw waveforms, the ratio between these two numbers, and the standard deviation of the differences between post-retracking SSHs and its one second averages for each retracker. In the whole test regions, there are 2,896,373 waveforms located at the sites with depth less than 200 m, which is about 19.83% of the total waveforms. The number of waveforms located at the sites deeper than 200 m is 11,708,222, which is about 80.17% of the total waveforms. Due to the complex reflection in the test regions, the percentage of reasonable SSH before retracking was only 94.72% (13,832,806 waveforms). After retracking, for most retrackers, more altimetry observations could be regarded as reasonable SSH. Such improvement in the validity of observation suggests that waveform retracking is an effective method to enhance the spatial resolution of altimetry data, especially with the complex waveforms. Compared with other retrackers, our new improved retracker presents the best performance in retrieving those "wrong" data, labeled before retracking. For an open ocean, the validity of observation with the new retracker increased from 94.81% to 95.40%; in shallow water, the validity of observation increased from 94.32% to 96.57%. The comparison of improvement in the validity of observation suggests that our improved retracker will retrieve more altimetry observations than what the other retrackers do.

Beside the increment of the validity of the observation, the improvement in precision of altimetry observation was also investigated by comparing the difference between post-retracking SSH and its average of 1 s for all retrackers. The comparison listed in Table 3 shows that the standard deviations of the differences for the case of raw SSHs and the cases of four retracked SSHs are 0.129, 0.155, 0.164, 0.156, and 0.138 m, respectively. In the coastal region, the return waveforms are complex and differ from classical ocean mode. Our new retracker gives the best performance in both improving data coverage (up to 96.57%) and precision (0.138 m). In the open ocean, the new retracker is still better in improving the data coverage (up to 95.40%). However, all retrackers will introduce new noise

Table 3
Performance of retrackers in the test regions (unit: m).

Total (14,604,595 waveforms)		Depth (>200 m) (11,708,222 waveforms)		Depth (10–200 m) (2,896,373 waveforms)	
Remove gross-errors	Noise std.	Number (%)	Noise std.	Number (%)	Noise std.
Raw[a] (13,832,806 waveforms)	0.129	11,100,958 (94.81)	0.122	2,731,848 (94.32)	0.155
Retracker I[b] (13,910,740 waveforms)	0.155	11,149,244 (95.23)	0.153	2,761,496 (95.34)	0.160
Retracker II[c] (13,821,314 waveforms)	0.164	11,044,944 (94.33)	0.166	2,776,370 (95.86)	0.154
Retracker III[d] (13,922,949 waveforms)	0.156	11,146,492 (95.20)	0.156	2,776,457 (95.86)	0.157
Retracker IV[e] (13,966,799 waveforms)	0.138	11,169,725 (95.40)	0.138	2,797,074 (96.57)	0.138

[a] Raw SSH.
[b] Beta-retracker.
[c] Improved threshold retracker.
[d] OCOG-retracker.
[e] Improved retracker.

to the raw SSHs, which may be derived from the algorithm for retracking gate and the uncertainty of return power of waveforms. Compared with other retrackers, the new retracker gives the least noise to the SSH determination (0.016 m). Given the waveform bin width 3.03 ns (for ERS), corresponding to 45.42 cm in the range, such a noise in retracked SSHs is statistically acceptable and could be reduced after being appropriately filtered along the track. The data reported in Table 3 also indicate that only our new retracker presents a uniform standard deviation (0.138) both for the open ocean and for the coastal regions, which means that we can employ this new retracker without considering the distribution of altimetry observations.

In terms of both coverage and precision of post-retracking SSHs, comparisons between retrackers confirm that the new improved retracking algorithm significantly outperforms the other retrackers.

From Table 3, it can be also found that the difference between retrackers in the deep seas is smaller than that in the coastal regions. A possible explanation is that in the deep seas, the return waveforms usually correspond well to the Brown model and all retrackers find the right leading edge, and the small difference might be derived from the algorithm for retracking gate; while in the coastal regions, the return waveforms are complex and differ from the classical ocean mode, some retrackers may fail to find the right leading edge, and the assumption in those retrackers based on the functional fit and statistic will not always be acceptable.

5. Conclusions

An improved retracking algorithm applicable to all altimeter waveforms, once there is a reasonable leading slope, was successfully constructed in this study. Without attempting to utilize a complicated model to explain the entire waveform, or to give statistical assumption on the adjacent waveforms, we reprocess each waveform separately. No previous referenced data were required. The new retracker is consistent with the physical process of waveform theory, so the post-retracking SSH is creditable and accurate. Compared with the existing retrackers in the experimental regions, the new approach gives the best performance both in an open ocean and in the coastal regions, and there is a significant improvement in the short-wavelength precision of the measurements and in the spatial resolution of sea surface height.

Future potential developments include the improvement of criteria in searching right slope and the algorithm for determining the retracking gate. We will reprocess the entire ERS and Geosat datasets, and produce a new global sea surface height with the improved algorithm, especially in the coastal regions.

Acknowledgements

This work was supported by the National Natural Science Foundation of China (Grant No. 40704005), High-Tech Research and Development Program of China (2006AA12Z128 and 2006AA12Z116) and the Knowledge Innovation Program of the Chinese Academy of Sciences (KZCX2-YW-125). The authors thank the NASA Physical Oceanography Distributed Active Archive Center and AVISO for the production and distribution of the altimeter waveform data.

References

[1] Fu LL, Cazenave A. Satellite altimetry and earth sciences. San Diego: Academic Press; 2001.
[2] Brown GS. The average impulse response of a rough surface and its applications. IEEE Trans Antenn Prop AP-25 1977;1:67–74.
[3] Mathers L, Berry PAM, Freeman JA. Gravity, geoid and space missions. In: International association of geodesy symposia, Porto, August 30–September 3, 2004.
[4] Deng XL, Featherstone WE, Hwang C, et al. Waveform retracking of ERS-1. Mar Geod 2002;251:189–204.
[5] Smith WHF, Sandwell DT. Improved global marine gravity field from reprocessing of Geosat and ERS-1 radar altimeter waveforms. In: AGU 2004 fall meeting, San Francisco; 2004.
[6] Andersen OB, Knudsen P, Berry PAM, et al. Initial results from retracking and reprocessing the ERS-1 geodetic mission altimeter for gravity field purposes. In: International association of geodesy symposia 2005, vol. 129; 2005. p. 1–5.
[7] Hwang C, Guo JY, Deng XL, et al. Coastal gravity anomalies from retracked geosat/GM altimetry: improvement, limitation and the role of airborne gravity data. J Geodesy 2006;804:204–16.
[8] Deng X, Featherstone WE. A coastal retracking system for satellite radar altimeter waveforms: application to ERS-2 around Australia. J Geophys Res 2006;111:C06012.
[9] Zwally HJ, Brenner AC. Ice sheet dynamics and mass balance. In: Satellite altimetry and earth sciences: a handbook of techniques and applications. San Diego: Academic Press; 2001.
[10] Guo JY, Hwang C, Deng XL, et al. Improved threshold retracker for satellite altimeter waveform retracking over coastal sea. Prog Natl Sci 2006;16(7):732–8.
[11] Garlick JD, Berry PAM, Mathers EL, et al. The Envisat/ERS river and lake retracking system. In: Proceedings of the 2004 Envisat & ERS symposium ESA SP-572, 6–10 September 2004, Salzburg, Austria; 2005 [published on CD-Rom, #348.1].
[12] Stewart RH. Methods of satellite oceanography. Berkley: University of California Press; 1985.
[13] Sandwell DT, Smith WHF. Retracking ERS-1 altimeter waveforms for optimal gravity field recovery. Geophys J Int 2005;163:79–89.
[14] Hayne GS. Radar altimeter mean waveforms from near-normal incidence ocean surface scattering. IEEE Trans Antenn Propag 1980;AP-28:687–92.
[15] Rodriguez E, Martin M. Estimation of the electromagnetic bias from retracked TOPEX data. J Geophys Res 1994;99(C12):24971–9.
[16] Davis CH. A robust threshold retracking algorithm for measuring ice-sheet surface elevation change from satellite radar altimeter. IEEE Trans Geosci Remote Sens 1997;354:974–9.
[17] Maus S, Green CM, Fairhead JD. Improved ocean-geoid resolution from retracked ERS-1 satellite altimeter waveforms. Geophys J Int 1998;134(N1):243–53.
[18] Martin TV, Zwally HJ, Brenner AC, et al. Analysis and retracking of continental ice sheet radar altimeter waveforms. J Geophys Res 1983;88:1608–16.
[19] Anzenhofer M, Shum CK, Rentsh M. Coastal altimetry and applications. Columbus, USA: Department of Geodesy Science and Surveying, Ohio State University; 1999. Report No. 464.
[20] Wingham DJ, Rapley CG, Griffiths H. New techniques in satellite tracking system. In: Proceedings of IGARSS' 88 symposium, Zurich; 1986. p. 1339–44.